ACS APPLIED MATERIALS & INTERFACES

Research Article

www.acsami.org

# An Improved Ultrasensitive Enzyme-Linked Immunosorbent Assay Using Hydrangea-Like Antibody–Enzyme–Inorganic Three-in-One Nanocomposites

Tianxiang Wei,[†,‡] Dan Du,[†] Mei-Jun Zhu,[§] Yuehe Lin,*[,†] and Zhihui Dai*[,‡]

[†]School of Mechanical and Materials Engineering, and [§]School of Food Science, Washington State University, Pullman, Washington 99164, United States

[‡]Jiangsu Collaborative Innovation Centre of Biomedical Functional Materials and Jiangsu Key Laboratory of Biofunctional Materials, School of Chemistry and Materials Science, Nanjing Normal University, Nanjing, 210023, P. R. China

Supporting Information

**ABSTRACT:** Protein–inorganic nanoflowers, composed of protein and copper(II) phosphate ($Cu_3(PO_4)_2$), have recently grabbed people's attention. Because the synthetic method requires no organic solvent and because of the distinct hierarchical nanostructure, protein–inorganic nanoflowers display enhanced catalytic activity and stability and would be a promising tool in biocatalytical processes and biological and biomedical fields. In this work, we first coimmobilized the enzyme, antibody, and $Cu_3(PO_4)_2$ into a three-in-one hybrid protein–inorganic nanoflower to enable it to possess dual functions: (1) the antibody portion retains the ability to specifically capture the corresponding antigen; (2) the nanoflower has enhanced enzymatic activity and stability to produce an amplified signal. The prepared antibody–enzyme–inorganic nanoflower was first applied in an enzyme-linked immunosorbent assay to serve as a novel enzyme-labeled antibody for *Escherichia coli* O157:H7 (*E. coli* O157:H7) determination. The detection limit is 60 CFU $L^{-1}$, which is far superior to commercial ELISA systems. The three-in-one antibody (anti-*E. coli* O157:H7 antibody)–enzyme (horseradish peroxidase)–inorganic ($Cu_3(PO_4)_2$) nanoflower has some advantages over commercial enzyme–antibody conjugates. First, it is much easier to prepare and does not need any complex covalent modification. Second, it has fairly high capture capability and catalytic activity because it is presented as aggregates of abundant antibodies and enzymes. Third, it has enhanced enzymatic stability compared to the free form of enzyme due to the unique hierarchical nanostructure.

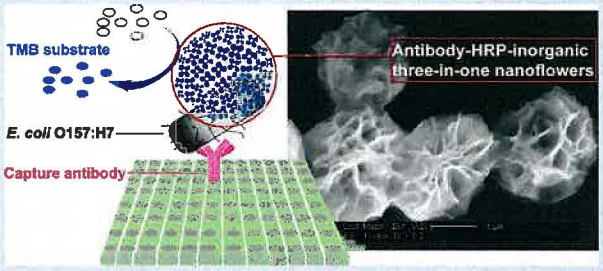


**KEYWORDS:** *ELISA, enzyme-labeled antibody, protein–inorganic nanoflower, ultrasensitive, E. coli O157:H7*

## INTRODUCTION

The enzyme-labeled antibody was established in the 1970s.[1,2] The high catalytic activity of enzymes enables the determination of trace amounts of target and greatly contributes to signal amplification. Enzyme-linked immunosorbent assay (ELISA), an immunodiagnostic technique developed by Engvall and Perlmann,[3] uses the enzyme-labeled antibody as one of its critical components. Since its development, ELISA has received widespread interest in application in the food industry, serological blood testing, and toxicology. Nowadays, ELISA holds a dominant position in the field of quantitative analysis because it is sensitive, selective, simple, and able to rapidly and simultaneously analyze a large number of samples. However, some limitations exist in its practical applications. Among all influence factors, the enzyme–antibody conjugate is the most critical reagent. The conventional enzyme-labeled antibody has relatively low sensitivity, and its main preparation methods, including the glutaraldehyde method and periodate method,[4] are relatively complicated and inefficient. This has been a bottleneck for ELISA in the recent ever-growing requirement toward low-abundance targets. Therefore, improved enzyme-labeled antibody methods for ELISA are much needed to meet the current demand.

Scientists have been making efforts to improve the conventional enzyme-labeled antibody method to achieve high sensitivity. For example, the biotin–streptavidin system utilizes the strept(avidin) and biotinylated protein to amplify the signal.[5,6] The immuno-PCR method combines the advantages of both ELISA and PCR to detect a low abundance of analytes.[7] Antibody-functionalized metallic nanocrystals consist of thousands to millions of metal atoms and can be dissolved into individual ions and produce large numbers of chromophores, to replace conventional enzymes for achieving high signal amplification.[8] The enzyme-loaded nanomaterial-labeled antibody has a high loading capacity for enzymes and shows remarkable signal amplification.[9−11] However, most of the above preparation methods are based on complex covalent immobilization, with an inevitable loss of enzyme activity.

Received: December 4, 2015
Accepted: February 19, 2016
Published: February 19, 2016





DOI: 10.1021/acsami.5b11834
ACS Appl. Mater. Interfaces 2016, 8, 6329–6335

**Scheme 1. Schematic Representation of the Hydrangea-Like Antibody–Enzyme–Inorganic Three-in-One Nanocomposite-Based Ultrasensitive ELISA for *E. coli* O157:H7 Detection**

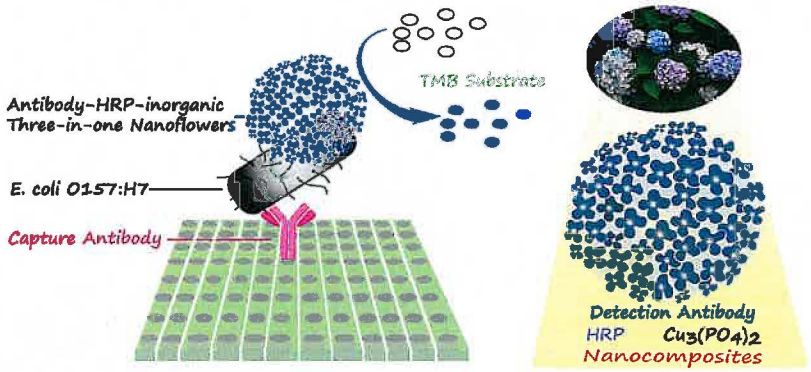


Recently, protein–inorganic hybrid nanoflowers made of protein and $Cu_3(PO_4)_2$ have attracted much attention since being first described by Richard Zare and co-workers.[12] Because of their simple preparation (one-step coprecipitation method) without any organic solvent, and distinct hierarchical nanostructure, the enzyme–inorganic nanoflowers showed greatly enhanced catalytic activity and stability.[13,14] This strategy of constructing protein–inorganic nanoflowers has provided a blueprint for other hybrid systems. For example, the glucose oxidase (GOx)–$Cu_3(PO_4)_2$ hybrid nanoflower has been applied to decompose organic pollutants efficiently,[15] the laccase–$Cu_3(PO_4)_2$ nanoflower was utilized to coat a membrane filter for rapid and on-site detection of phenol,[16] the derived $\alpha$-amylase–calcium hydrophosphate ($CaHPO_4$) hybrid nanoflowers displayed dramatically enhanced enzymatic performance with a distinct $Ca^{2+}$-assisted allosteric effect from $\alpha$-amylase,[17] and the bovine serum albumin (BSA)–manganese phosphate ($Mn_3(PO_4)_2$) hybrid was first applied as a carrier for the loading of platinum nanoparticles (PtNPs) and the composite served as a high-efficiency Pt-based catalyst.[18] In addition, multienzyme-coembedded organic–inorganic hybrid nanoflowers (GOx and HRP–$Cu_3(PO_4)_2$ nanoflowers) were prepared, which were able to achieve a one-step two-enzyme cascade catalytic reaction.[19] There are also a few other works related to protein–inorganic nanoflowers.[14,20−23] According to recent developments, protein–inorganic nanoflowers would be a promising tool in biomedical fields, in biocatalytical processes, and even in electrochemical catalysis. However, the above studies were restricted to only one kind of protein, the enzyme.

In this work, we first coimmobilized the enzyme, antibody, and $Cu_3(PO_4)_2$ into a three-in-one hybrid antibody–protein–inorganic nanoflower. The cooperation of enzyme and antibody conveys dual functions to the nanoflower: the specific capture ability toward the corresponding antigen and the enhanced enzymatic activity and stability for producing an amplified signal. The prepared antibody–enzyme–inorganic three-in-one nanoflower was further applied in ELISA to serve as a novel enzyme-labeled antibody. *E. coli* O157:H7 is an important foodborne pathogen, which can cause serious infection in low doses.[24−28] Therefore, we chose *E. coli* O157:H7 as a model analyte. The enzyme–antibody–inorganic three-in-one nanoflower shows advantages over the commercial enzyme-labeled antibody. First, it is much easier to prepare with no need for any complex covalent modification. Second, it is an aggregate of numbers of antibodies and enzymes, so it has fairly high captive ability and catalytic activity. Furthermore, it has enhanced enzymatic stability compared to their free form due to its unique hierarchical nanostructure. It is highly expected that these three-in-one nanoflowers will ultimately have significant practical applications. The antibody–enzyme–inorganic nanoflower-based ELISA immunoassay procedure for *E. coli* O157 determination is illustrated in Scheme 1.

## EXPERIMENTAL SECTION

**Reagents and Materials.** *E. coli* O157:H7 and other foodborne pathogens such as *Salmonella* and *Listeria monocytogenes* were kindly provided by Prof. Zhu at Washington State University. Mouse monoclonal anti-*E. coli* O157:H7 antibody (capture antibody/$Ab_1$) was purchased from Abcam (Cambridge, MA). Goat polyclonal anti-*E. coli* O157:H7 antibody (detection antibody/$Ab_2$) was purchased from KPL Inc. (Gaithersburg, MD). Horseradish peroxidase (HRP), bovine serum albumin (BSA), copper(II) sulfate pentahydrate ($CuSO_4 \cdot 5H_2O$), 3,3′,5,5′-tetramethylbenzidine (TMB) liquid substrate system for ELISA, phosphate-buffered saline (0.01 M phosphate buffer, 0.0027 M potassium chloride and 0.137 M sodium chloride, pH 7.4, at 25 °C), Tween 20, and potassium chloride were purchased from Sigma-Aldrich (USA). ELISA 96-well flat-bottom plates (Corning no. 9018) were purchased from Fisher Scientific (Pittsburgh, PA). All aqueous solutions were prepared using ultrapure water (18.2 MΩ cm) as required.

***E. coli* O157:H7 Sample Preparation.** *E. coli* O157:H7 EDL933 was obtained from the STEC Center at Michigan State University. The *E. coli* O157:H7 cultures were activated in Luria–Bertani (LB) broth and washed with 0.01 M PBS, pH 7.0. A portion of washed *E. coli* O157:H7 suspension was 10-fold serial diluted and plated onto LB agar plates for cell enumeration. The rest of the *E. coli* O157:H7 suspension was heat treated, 0.5% (v/v) formalin added and mixed, and the mixture stored at −20 °C until analysis.

**Preparation of Antibody–Enzyme–Inorganic Nanoflowers.** The antibody–enzyme–inorganic nanoflowers were synthesized according to the one-step coprecipitation method reported by Zare's lab[12] with some modifications. Typically, 120 μL of aqueous $CuSO_4$ solution (100 mM) was added to 13.805 mL of $H_2O$, 750 μL of 0.01 M PBS (pH 7.4), and 100 μL of 10% KCl solution containing 150 μL of HRP (1 mg $mL^{-1}$) and 75 μL of $Ab_2$ (2 mg $mL^{-1}$), followed by incubation at 25 °C for 18 h. The scanning electron microscopy (SEM) samples were prepared by dripping a dilute aqueous dispersion of the as-prepared samples directly onto the conductive adhesive. The three-in-one nanoflower precipitate was collected through centrifugation (5000 rpm, 10 min), washed with deionized water, freeze-dried, and stored at −20 °C. The nanoflowers were resuspended in PBS (50 μg $mL^{-1}$) by mildly vortexing. Then the solution was separated into small aliquots and stored at −20 °C before use.

**Sandwich Three-in-one Nanoflower-Based ELISA of *E. coli* O157:H7.** A 100 μL amount of 6 μg $mL^{-1}$ $Ab_1$ diluted in 0.05 M carbonate buffer solution (pH 9.6) was added to a 96-well plate and incubated at 4 °C for 12 h. The plate was then aspirated and rinsed with 300 μL of PBST (0.05% Tween 20 in 0.01 M PBS) for each well



DOI: 10.1021/acsami.5b11834
ACS Appl. Mater. Interfaces 2016, 8, 6329−6335

four times to remove unbound antibodies, and the liquid was completely removed by inverting the plate and blotting it against clean paper towels. Afterward, 300 μL of PBSA (1% BSA in 0.01 M PBS) was added, incubated at 37 °C for 40 min, and washed. Then 100 μL of *E. coli* O157:H7 suspension at different concentrations was added to each well and incubated at 37 °C for 45 min. After washing four times, 100 μL of 8 μg $mL^{-1}$ HRP–$Ab_2$–$Cu_3(PO_4)_2$ nanocomposite was added to each well and incubated at 37 °C for 40 min. The plate was washed five times to remove unbound HRP–$Ab_2$–$Cu_3(PO_4)_2$ nanocomposite. Finally, 100 μL of TMB liquid substrate system for ELISA was added to each well and incubated at 37 °C for 20 min. The reaction was terminated using 50 μL of 2 N $H_2SO_4$, and the optical density of each well was determined within 30 min, using a Tecan Safire 2 microplate reader (Tecan, Switzerland) set to 450 nm with a wavelength correction of 540 nm.

## RESULTS AND DISCUSSION

**Morphology Characterization of the Three-in-One Nanoflowers.** SEM images of the HRP–$Ab_2$–$Cu_3(PO_4)_2$ nanoflowers with the magnifications from low to high are shown in Figure 1. In the low-resolution SEM image, most of

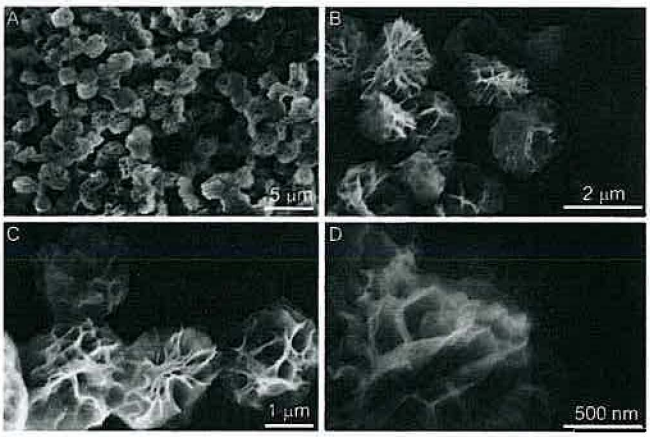


**Figure 1.** SEM images showing the morphologies of anti-*E. coli* O157:H7 antibody–HRP–$Cu_3(PO_4)_2$ three-in-one nanoflowers with magnifications from low to high (A–D).

the HRP–$Ab_2$–$Cu_3(PO_4)_2$ nanoflowers look like hydrangeas with a uniform size of approximately 2 μm (Figure 1A). The higher-resolution images of HRP–$Ab_2$–$Cu_3(PO_4)_2$ nanoflowers show that they have hierarchical structures with high surface-to-volume ratios, which really seem like they are assembled from hundreds of nanopetals (Figure 1B–D). As elaborated by Jie Zeng and Younan Xia,[29] the high surface area of the porous nanoflowers, the cooperative effects of the nanoscale-entrapped protein molecules, and the coordination between the amino acid residues of proteins and $Cu^{2+}$ endow the nanoflowers with enhanced stability and activity.

The stability of the antibody–HRP–$Cu_3(PO_4)_2$ nanoflower was further compared with that of the free HRP. The nanoflowers maintained ~93% of their catalytic activity after 10 days of storage in PBS at room temperature while the free HRP only retained ~47% of its original catalytic activity (Figure 2A). Furthermore, morphologies of the nanoflowers had little change even after being stored in PBS for two months (Figure 2B). The above results indicated the good stability of the nanoflowers.

**Optimization of Detection Conditions for Three-in-One Nanoflower-Based ELISA.** A variety of factors can affect ELISA performance. Herein, the optical densities of the control group (0 CFU $mL^{-1}$ *E. coli* O157:H7) and experimental group ($1.7 \times 10^6$ CFU $mL^{-1}$ *E. coli* O157:H7) were investigated simultaneously for evaluating the effects of four factors on detection sensitivity: the concentration of capture antibody, the concentration of blocking agent–BSA, the concentration of detection antibody (HRP–$Ab_2$–$Cu_3(PO_4)_2$ nanoflowers), and the incubation time of detection antibody. As shown in Figure 3A, with increasing the concentration of $Ab_1$ from 1.0 to 7.0 μg $mL^{-1}$, the OD value of the experimental group kept increasing until 6.0 μg $mL^{-1}$ of $Ab_1$, indicating that 6.0 μg $mL^{-1}$ of $Ab_1$ coating is already sufficient and saturated for antigen binding. Hence, a concentration of 6.0 μg $mL^{-1}$ of $Ab_1$ was chosen to coat the 96-well plate. The concentration of blocking agent–BSA is also an important parameter for ELISA performance. Figure 3B shows that the OD value of the experimental group decreased with increasing concentration of BSA and tended to level off after 1% BSA, and the OD value of control group showed false-positive results before 1% BSA, which is probably attributed to the fact that insufficient blocking agent might result in nonspecific interaction of the detection antibody. Therefore, 1% BSA was selected as the appropriate concentration of blocking agent. Figure 3C shows that the concentration of detection antibody is another critical parameter. The OD value of the experimental group increased with increasing concentration of the HRP–$Ab_2$–$Cu_3(PO_4)_2$ nanoflowers, while the OD value of the control group began to yield false-positive results when adding 8 μg $mL^{-1}$ or more of HRP–$Ab_2$–$Cu_3(PO_4)_2$ nanoflowers. Therefore, 8 μg $mL^{-1}$ was selected as an appropriate concentration of HRP–$Ab_2$–

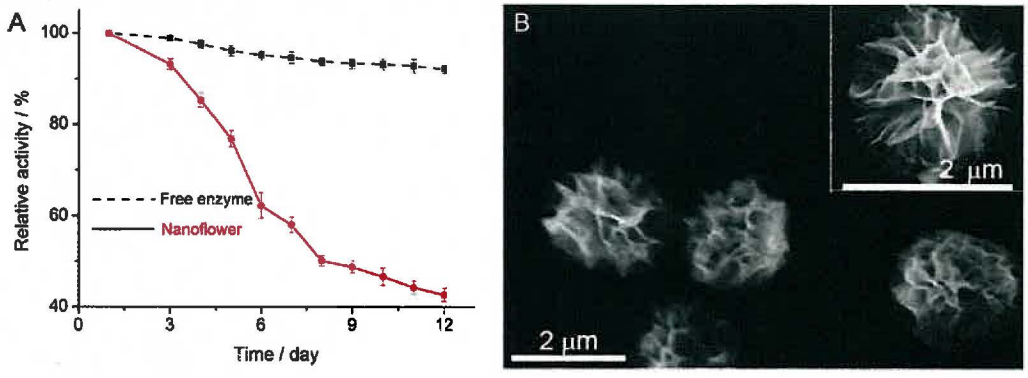


**Figure 2.** Storage stability of antibody–HRP–$Cu_3(PO_4)_2$ nanoflowers. (A) The enzymatic activity of nanoflowers and free HRP in PBS (pH 7.4) during storage at room temperature. (B) SEM images of the nanoflowers stored in PBS for two months.



DOI: 10.1021/acsami.5b11834
ACS Appl. Mater. Interfaces 2016, 8, 6329–6335

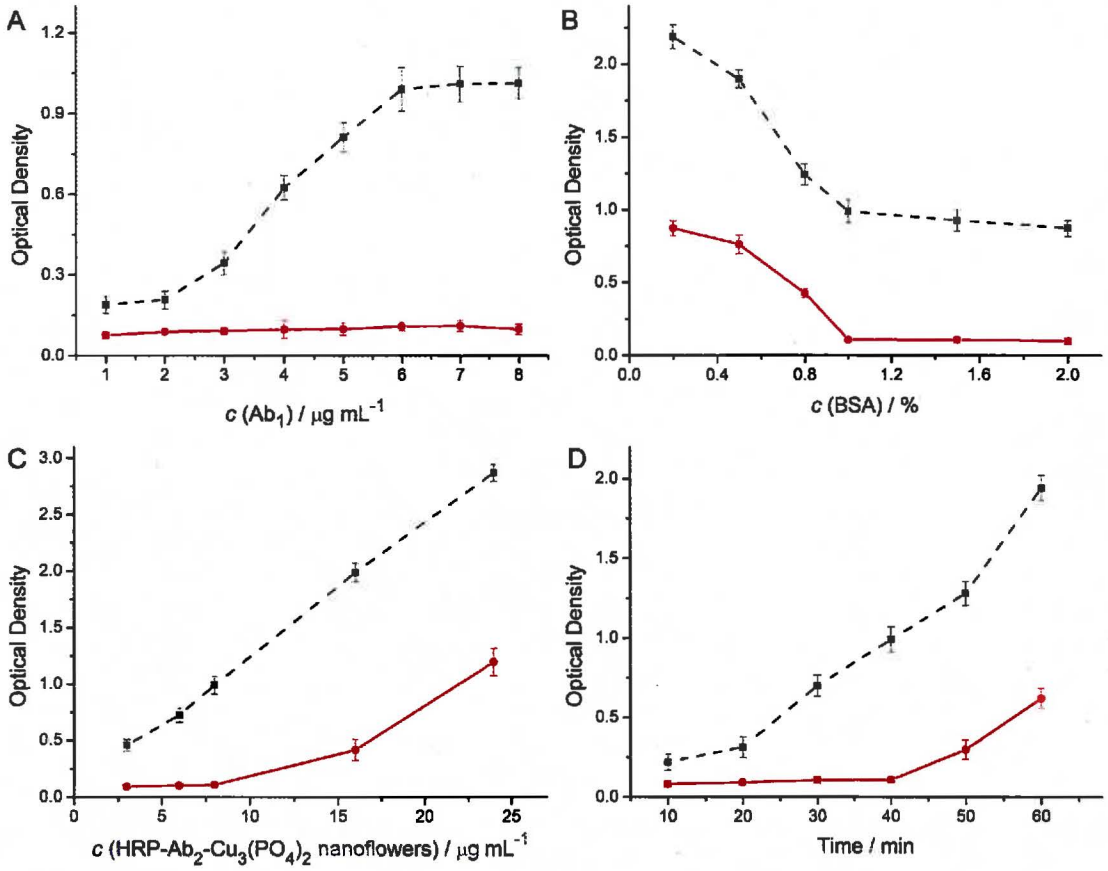


**Figure 3.** Optimization of ELISA detection conditions. (A) The concentration of capture antibody ($Ab_1$), (B) the concentration of BSA, (C) the concentration of the HRP–$Ab_2$–$Cu_3(PO_4)_2$ nanoflowers, and (D) incubation time of the HRP–$Ab_2$–$Cu_3(PO4)_2$ nanoflowers. The solid and dashed lines mean the optical densities obtained from the assays without or with $1.7 \times 10^6$ CFU $mL^{-1}$ *E. coli* O157:H7, respectively.

$Cu_3(PO_4)_2$ nanoflowers. ELISA performance was also related to the incubation time of detection antibody. As revealed in Figure 3D, the OD value of the control group produced false positive results after 40 min incubation time of HRP–$Ab_2$–$Cu_3(PO_4)_2$ nanoflowers. This is because longer incubation time of the antibody may lead to more nonspecific binding. Therefore, the optimal incubation time of detection antibody was 40 min.

**Performance of the Three-in-One Nanoflower-Based ELISA for *E. coli* O157:H7.** Under the above optimized conditions, the three-in-one nanoflower-based ELISA system was used to quantitatively determine the concentrations of the *E. coli* O157:H7. The binding feasibility between antibody–HRP–$Cu_3(PO_4)_2$ nanoflower and *E. coli* O157:H7 was verified through the SEM images (Figure S1, Supporting Information). From the ELISA quantitative results (Figure 4A), the OD value increased with the increasing concentration of *E. coli* O157:H7. The calibration curve between the OD value and the concentration of *E. coli* O157:H7 is shown in Figure 4B, which reveals that the OD increment was highly sensitive to the concentration of *E. coli* O157:H7 and demonstrates that our hydrangea-like antibody–enzyme–inorganic three-in-one nanocomposite-based ELISA could provide a quantitative measurement of *E. coli* O157:H7 over $1.7 \times 10^1$ to $1.7 \times 10^7$ CFU $mL^{-1}$ with an ultrasensitive detection limit of 60 CFU $L^{-1}$. The detection limit is defined as the concentration of the analyte at which the extrapolated linear portion of the calibration graph intersects the baseline of the means of data from blank tests (Compendium of Chemical Terminology, IUPAC). This is better than most of the reported research results for quantitative determination of *E. coli* O157:H7 (Table 1) or comparable with the sensitive *E. coli* O157:H7 assay via new and sophisticated technology such as long-range surface plasmon-enhanced fluorescence spectroscopy (LSPFS).[30] These results indicated enhanced action of the antibody–enzyme–inorganic nanoflowers compared with the common HRP-conjugated antibody.

Specificity, stability, and recovery are important assessment criteria for the ELISA detection method. To assess the specificity of the nanoflower-based ELISA for *E. coli* O157:H7, we compared its specificity for nonpathogenic generic *E. coli* K12 and other foodborne pathogens such as *Salmonella* and *Listeria monocytogenes*. The OD values for other bacteria are roughly the same with the control group, while *E. coli* O157:H7 or culture mixtures give a high OD value (Figure 5A). These results suggested that the developed nanoflower-based ELISA for *E. coli* O157:H7 is specific to *E. coli* O157:H7.

The stability of the three-in-one nanoflower was further tested in the *E. coli* O157:H7 ELISA. Two test samples with different concentrations of *E. coli* O157:H7 ($1.7 \times 10^5$ CFU $mL^{-1}$ and $1.7 \times 10^6$ CFU $mL^{-1}$) were assayed using the same lot of HRP–$Ab_2$–$Cu_3(PO_4)_2$ nanocomposites over a 40 day period. The ELISA performance shown in Figure 5B indicated the acceptable stability of the antibody–enzyme–inorganic nanoflowers and its potential to substitute for common existing enzyme-conjugated antibodies in ELISA systems. Recovery experiments are used to determine whether assays are affected by interfering factors. Different concentrations of *E. coli* O157:H7 were spiked into tap water and lake water and then


DOI: 10.1021/acsami.5b11834
ACS Appl. Mater. Interfaces 2016, 8, 6329–6335

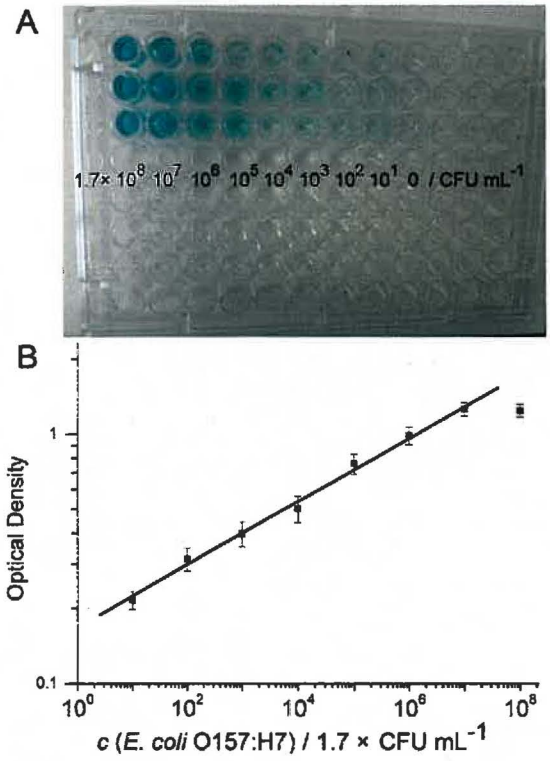


**Figure 4.** (A) A representative image of the new enzyme-labeled antibody method-based ELISA strips. (B) *E. coli* O157:H7 was quantified with a sandwich HRP–$Ab_2$–$Cu_3(PO_4)_2$ nanoflower-based ELISA. Mean ± standard deviation of three measurements is plotted. The optical density of each well was read at 450 nm with a wavelength correction of 540 nm. Each experiment was repeated three times to obtain the average data value.

**Table 1. Comparison of the Performance of Different *E. coli* O157:H7 Assays**[a]

| bacterium | technique | linear range (CFU $mL^{-1}$) | LOD (CFU $mL^{-1}$) | reference |
|---|---|---|---|---|
| *E. coli* O157:H7 | chemiluminescence immunoassay | $4.3 \times 10^3$ to $4.3 \times 10^5$ | $1.2 \times 10^3$ | 31 |
| *E. coli* O157:H7 | LSPFS | $10^1$ to $10^6$ | 10 | 30 |
| *E. coli* O157:H7 | electrochemical ELISA | $10^3$ to $10^8$ | $10^3$ | 32 |
| *E. coli* O157:H7 | amperometric immunosensor | $3.6 \times 10^3$ to $3.6 \times 10^6$ | $4.3 \times 10^2$ | 33 |
| *E. coli* O157:H7 | electrochemical impedance spectroscopy | $10^3$ to $10^7$ | $10^3$ | 34 |
| *E. coli* O157:H7 | electrochemical biosensor | $10^2$ to $10^5$ | $10^2$ | 35 |
| *E. coli* O157:H7 | gold nanoparticle-enhanced ELISA | $10^2$ to $10^8$ | 68 | 36 |
| *E. coli* O157:H7 | antibody–gold nanoparticle network ELISA | $10^1$ to $10^5$ | 3 | 37 |
| *E. coli* O157:H7 | ConA-HRP–carbon nanotube-based ELISA | $10^2$ to $10^5$ | 100 | 38 |
| *E. coli* O157:H7 | three-in-one nanoflower-based ELISA | $1.7 \times 10^1$ to $1.7 \times 10^7$ | 0.06 | this work |

[a]ELISA: enzyme-linked immunosorbent assay; LOD: level of detection; LSPFS: long-range surface plasmon-enhanced fluorescence spectroscopy.

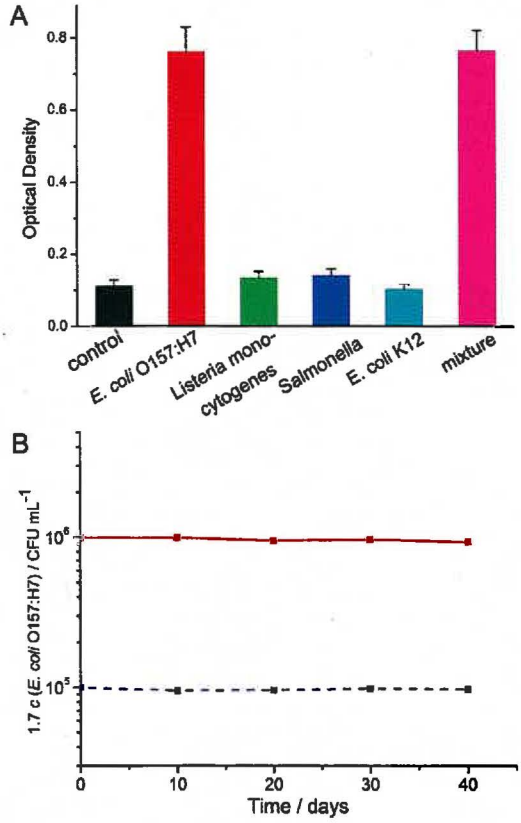


**Figure 5.** (A) Optical density of the anti-*E. coli* O157:H7 antibody–HRP–$Cu_3(PO_4)_2$ nanoflower-based ELISA after incubation with different bacteria ($1.7 \times 10^5$ CFU $mL^{-1}$). (B) Two samples with different concentrations of *E. coli* O157:H7 were assayed using the same lot of the HRP–$Ab_2$–$Cu_3(PO_4)_2$ nanocomposites over a 40 day period.

analyzed for recovery. The results showed that recoveries were in the range of 92.9–101.8% (Table 2), which confirmed the high accuracy of the nanoflower-based ELISA and its great potential for practical application in the detection of *E. coli* O157:H7 in water.

**Table 2. Recoveries for *E. coli* O157:H7-Spiked Samples**

| sample | added (CFU $mL^{-1}$) | found (CFU $mL^{-1}$) | recovery (%) |
|---|---|---|---|
| tap water 1 | $1.7 \times 10^2$ | $1.65 \times 10^2$ | 97.6 |
| tap water 2 | $1.7 \times 10^4$ | $1.72 \times 10^4$ | 101.8 |
| tap water 3 | $1.7 \times 10^6$ | $1.63 \times 10^6$ | 96.4 |
| lake water 1 | 0 | not detectable | — |
| lake water 2 | $1.7 \times 10^2$ | $1.58 \times 10^2$ | 92.9 |
| lake water 3 | $1.7 \times 10^4$ | $1.61 \times 10^4$ | 94.7 |

## CONCLUSIONS

For the first time, we developed a hydrangea-like antibody–enzyme–inorganic three-in-one nanocomposite as a novel enzyme-labeled antibody and applied it to ELISA for detection of *E. coli* O157:H7. The antibody–enzyme–inorganic nanoflower is simply synthesized by a one-step coprecipitation method and does not require any organic solvent. It has the function of an antibody to specifically interact with the corresponding antigen and also has enhanced enzymatic activity and stability. The anti-*E. coli* O157:H7 antibody–HRP–$Cu_3(PO_4)_2$ nanocomposite was used to replace the common



DOI: 10.1021/acsami.5b11834
ACS Appl. Mater. Interfaces 2016, 8, 6329–6335

HRP-conjugated antibody and was applied in the ELISA for *E. coli* O157:H7 determination. The results showed that the three-in-one nanoflower-based *E. coli* O157:H7 ELISA had an ultrasensitive performance with a wide detection range ($1.7 \times 10^1$ to $1.7 \times 10^7$ CFU $mL^{-1}$). The detection limit is far superior to that of commercial ELISA systems. The easy preparation of these nanocomposites and the ultrasensitive detection of *E. coli* O157:H7 show potential application in real samples. Furthermore, the strategy of making antibody–enzyme–inorganic nanoflowers as described in this work can be readily extended to many other hybrid systems. For example, different antibodies could serve as components in nanoflower preparation to expand the use of antibody–enzyme–inorganic nanoflower-based ELISA to the detection of various targets. In addition, enzymes other than HRP could be used in nanoflowers that would not require colorimetric assay but rather an alternative mode of detection depending on the enzyme chosen. The methodology proposed here could potentially replace the common existing enzyme-labeled antibody method in ELISA and will have significant prospects in the practical detection of other pathogenic bacteria or clinically relevant molecules.

## ■ ASSOCIATED CONTENT

### Supporting Information

The Supporting Information is available free of charge on the ACS Publications website at DOI: 10.1021/acsami.5b11834.

SEM images of *E. coli* O157:H7 and the binding status between anti-*E. coli* O157:H7 antibody–HRP–$Cu_3(PO_4)_2$ nanoflowers and *E. coli* O157:H7 (PDF)

## ■ AUTHOR INFORMATION


### Corresponding Authors

*E-mail: daizhihuii@njnu.edu.cn.

*E-mail: Yuehe.lin@wsu.edu.


### Notes

The authors declare no competing financial interest.

## ■ ACKNOWLEDGMENTS

This work was partly supported by the Centers for Disease Control and Prevention/National Institute for Occupational Safety and Health (CDC/NIOSH) grant no. R21OH010768. Its contents are solely the responsibility of the authors and do not necessary represent the official views of CDC. T.W. acknowledges the support of China Scholarship Council (No. 201406860004).

## ■ REFERENCES


(1) Graham, R. C., Jr.; Karnovsky, M. J. The Early Stages of Absorption of Injected Horseradish Peroxidase in the Proximal Tubules of Mouse Kidney: Ultrastructural Cytochemistry by a New Technique. *J. Histochem. Cytochem.* **1966**, *14*, 291–302.

(2) Ram, J. S.; Nakane, P. K.; Rawlinson, D. G.; Pierce, G. B. Enzyme Labelled Antibodies for Ultrastructural Studies. *Fed. Proc.* **1966**, *25*, 732–738.

(3) Engvall, E.; Perlmann, P. Enzyme-linked Immunosorbent assay (ELISA). Quantitative Assay of Immunoglobulin G. *Immunochemistry* **1971**, *8*, 871–874.

(4) Jeanson, A.; Cloes, J. M.; Bouchet, M.; Rentier, B. Comparison of Conjugation Procedures for the Preparation of Monoclonal Antibody-Enzyme Conjugates. *J. Immunol. Methods* **1988**, *111*, 261–270.

(5) Chu, Y. W.; Wang, B. Y.; Lin, H. S.; Lin, T. Y.; Hung, Y. J.; Engebretson, D. A.; Lee, W.; Carey, J. R. Layer by Layer Assembly of Biotinylated Protein Networks for Signal Amplification. *Chem. Commun.* **2013**, *49*, 2397–2399.

(6) Hsu, S. M.; Raine, L.; Fanger, H. The Use of Avidinbiotin Peroxidase Complex (ABC) in Immunoperoxidase Techniques: A Comparison Between ABC and Unlabeled Antibody (PAP) Procedures. *J. Histochem. Cytochem.* **1981**, *29*, 577–580.

(7) Malou, N.; Raoult, D. Immuno-PCR: A Promising Ultrasensitive Diagnostic Method to Detect Antigens and Antibodies. *Trends Microbiol.* **2011**, *19*, 295–302.

(8) Tong, S.; Ren, B. B.; Zheng, Z. L.; Shen, H.; Bao, G. Tiny Grains Give Huge Gains: Nanocrystal-Based Signal Amplification for Biomolecule Detection. *ACS Nano* **2013**, *7*, 5142–5150.

(9) Lin, H.; Liu, Y.; Huo, J.; Zhang, A.; Pan, Y.; Bai, H.; Jiao, Z.; Fang, T.; Wang, X.; Cai, Y.; Wang, Q.; Zhang, Y.; Qian, X. Modified Enzyme-linked Immunosorbent Assay Strategy Using Graphene Oxide Sheets and Gold Nanoparticles Functionalized with Different Antibody Types. *Anal. Chem.* **2013**, *85*, 6228–6232.

(10) Qu, Z. Y.; Xu, H.; Xu, P.; Chen, K. M.; Mu, R.; Fu, J. P.; Gu, H. C. Ultrasensitive ELISA Using Enzyme-Loaded Nanospherical Brushes as Labels. *Anal. Chem.* **2014**, *86*, 9367–9371.

(11) Su, J.; Xu, J.; Chen, Y.; Xiang, Y.; Yuan, R.; Chai, Y. Q. Personal Glucose Sensor for Point-of-Care Early Cancer Diagnosis. *Chem. Commun.* **2012**, *48*, 6909–6911.

(12) Ge, J.; Lei, J.; Zare, R. N. Protein–Inorganic Hybrid Nanoflowers. *Nat. Nanotechnol.* **2012**, *7*, 428–432.

(13) Zhang, Y. F.; Ge, J.; Liu, Z. Enhanced Activity of Immobilized or Chemically Modified Enzymes. *ACS Catal.* **2015**, *5*, 4503–4513.

(14) Yin, Y. Q.; Xiao, Y.; Lin, G.; Xiao, Q.; Lin, Z.; Cai, Z. W. An Enzyme–Inorganic Hybrid Nanoflower Based Immobilized Enzyme Reactor with Enhanced Enzymatic Activity. *J. Mater. Chem. B* **2015**, *3*, 2295–2300.

(15) Huang, Y. Y.; Ran, X.; Lin, Y. H.; Ren, J. S.; Qu, X. G. Self-assembly of an Organic–inorganic Hybrid Nanoflower as an Efficient Biomimetic Catalyst for Self-Activated Tandem Reactions. *Chem. Commun.* **2015**, *51*, 4386–4389.

(16) Zhu, L.; Gong, L.; Zhang, Y. F.; Wang, R.; Ge, J.; Liu, Z.; Zare, R. N. Rapid Detection of Phenol Using a Membrane Containing Laccase Nanoflowers. *Chem. - Asian J.* **2013**, *8*, 2358–2360.

(17) Wang, L. B.; Wang, Y. C.; He, R.; Zhuang, A.; Wang, X. P.; Zeng, J.; Hou, J. G. A New Nanobiocatalytic System Based on Allosteric Effect with Dramatically Enhanced Enzymatic Performance. *J. Am. Chem. Soc.* **2013**, *135*, 1272–1275.

(18) Zhang, Z. H.; Zhang, Y. C.; He, L. H.; Yang, Y. Q.; Liu, S. L.; Wang, M. H.; Fang, S. M.; Fu, G. D. A Feasible Synthesis of $Mn_3(PO_4)_2$@BSA Nanoflowers and Its Application as the Support Nanomaterial for Pt Catalyst. *J. Power Sources* **2015**, *284*, 170–177.

(19) Sun, J. Y.; Ge, J. C.; Liu, W. M.; Lan, M. H.; Zhang, H. Y.; Wang, P. F.; Wang, Y. M.; Niu, Z. W. Multi-enzyme Co-embedded Organic–inorganic Hybrid Nanoflowers: Synthesis and Application as a Colorimetric Sensor. *Nanoscale* **2014**, *6*, 255–262.

(20) Li, Z.; Zhang, Y.; Su, Y.; Ouyang, P.; Ge, J.; Liu, Z. Spatial Co-localization of Multi-enzymes by Inorganic Nanocrystal-Protein Complexes. *Chem. Commun.* **2014**, *50*, 12465–12468.

(21) Lin, Z.; Xiao, Y.; Wang, L.; Yin, Y. Q.; Zheng, J. N.; Yang, H. H.; Chen, G. N. Facile Synthesis of Enzyme–Inorganic Hybrid Nanoflowers and Their Application as an Immobilized Trypsin Reactor for Highly Efficient Protein Digestion. *RSC Adv.* **2014**, *4*, 13888–13891.

(22) Lin, Z.; Xiao, Y.; Yin, Y. Q.; Hu, W. L.; Liu, W.; Yang, H. H. Facile Synthesis of Enzyme-Inorganic Hybrid Nanoflowers and Its Application as a Colorimetric Platform for Visual Detection of Hydrogen Peroxide and Phenol. *ACS Appl. Mater. Interfaces* **2014**, *6*, 10775–10782.

(23) Wang, X. L.; Shi, J. F.; Li, Z.; Zhang, S. H.; Wu, H.; Jiang, Z. Y.; Yang, C.; Tian, C. Y. Facile One-Pot Preparation of Chitosan/Calcium Pyrophosphate Hybrid Microflowers. *ACS Appl. Mater. Interfaces* **2014**, *6*, 14522–14532.

(24) Perna, N. T.; Plunkett, G.; Burland, V.; Mau, B.; Glasner, J. D.; Rose, D. J.; Mayhew, G. F.; Evans, P. S.; Gregor, J.; Kirkpatrick, H. A.; Posfai, G.; Hackett, J.; Klink, S.; Boutin, A.; Shao, Y.; Miller, L.;




DOI: 10.1021/acsami.5b11834
ACS Appl. Mater. Interfaces 2016, 8, 6329–6335

Grotbeck, E. J.; Davis, N. W.; Lim, A.; Dimalanta, E. T.; Potamousis, K. D.; Apodaca, J.; Anantharaman, T. S.; Lin, J. Y.; Yen, G.; Schwartz, D. C.; Welch, R. A.; Blattner, F. R. Genome Sequence of Enterohaemorrhagic Escherichia coli O157:H7. *Nature* **2001**, *409*, 529−533.

(25) Radke, S. A.; Alocilja, E. C. A High Density Microelectrode Array Biosensor for Detection of E-coli O157:H7. *Biosens. Bioelectron.* **2005**, *20*, 1662−1667.

(26) Eppinger, M.; Mammel, M. K.; Leclerc, J. E.; Ravel, J.; Cebula, T. A. Genomic Anatomy of Escherichia coli O157:H7 Outbreaks. *Proc. Natl. Acad. Sci. U. S. A.* **2011**, *108*, 20142−20147.

(27) Scallan, E.; Hoekstra, R. M.; Angulo, F. J.; Tauxe, R. V.; Widdowson, M. A.; Roy, S. L.; Jones, J. L.; Griffin, P. M. Foodborne Illness Acquired in the United States-Major Pathogens. *Emerging Infect. Dis.* **2011**, *17*, 7−15.

(28) Tarr, P. I. Escherichia coli O157:H7: Clinical, Diagnostic, and Epidemiological Aspects of Human Infection. *Clin. Infect. Dis.* **1995**, *20*, 1−8.

(29) Zeng, J.; Xia, Y. N. Hybrid Nanomaterials: Not Just a Pretty Flower. *Nat. Nanotechnol.* **2012**, *7*, 415−416.

(30) Huang, C. J.; Dostalek, J.; Sessitsch, A.; Knoll, W. Long-range Surface Plasmon-enhanced Fluorescence Spectroscopy Biosensor for Ultrasensitive Detection of *E. coli* O157:H7. *Anal. Chem.* **2011**, *83*, 674−677.

(31) Zhang, Y.; Tan, C.; Fei, R. H.; Liu, X. X.; Zhou, Y.; Chen, J.; Chen, H. C.; Zhou, R.; Hu, Y. G. Sensitive Chemiluminescence Immunoassay for *E. coli* O157:H7 Detection with Signal Dual-Amplification Using Glucose Oxidase and Laccase. *Anal. Chem.* **2014**, *86*, 1115−1122.

(32) Akanda, M. R.; Tamilavan, V.; Park, S.; Jo, K.; Hyun, M. H.; Yang, H. Hydroquinone Diphosphate as a Phosphatase Substrate in Enzymatic Amplification Combined with Electrochemical-Chemical-Chemical Redox Cycling for the Detection of *E. coli* O157:H7. *Anal. Chem.* **2013**, *85*, 1631−1636.

(33) Cheng, P.; Huang, Z. G.; Zhuang, Y.; Fang, L. C.; Huang, H.; Deng, J.; Jiang, L. L.; Yu, K. K.; Li, Y.; Zheng, J. S. A Novel Regeneration-free E. coli O157:H7 Amperometric Immunosensor Based on Functionalised Four-Layer Magnetic Nanoparticles. *Sens. Actuators, B* **2014**, *204*, 561−567.

(34) Li, Y.; Afrasiabi, R.; Fathi, F.; Wang, N.; Xiang, C.; Love, R.; She, Z.; Kraatz, H. B. Impedance Based Detection of Pathogenic *E. coli* O157:H7 Using a Ferrocene-Antimicrobial Peptide Modified Biosensor. *Biosens. Bioelectron.* **2014**, *58*, 193−199.

(35) Hassan, A. R. H. A. A.; de la Escosura-Muniz, A.; Merkoci, A. Highly Sensitive and Rapid Determination of Escherichia coli O157:H7 in Minced Beef and Water Using Electrocatalytic Gold Nanoparticle Tags. *Biosens. Bioelectron.* **2015**, *67*, 511−515.

(36) Shen, Z. Q.; Hou, N. A.; Jin, M.; Qiu, Z. G.; Wang, J. F.; Zhang, B.; Wang, X. W.; Wang, J.; Zhou, D. S.; Li, J. W. A Novel Enzyme-linked Immunosorbent Assay for Detection of Escherichia coli O157:H7 Using Immunomagnetic and Beacon Gold Nanoparticles. *Gut Pathog.* **2014**, *6*, 14 10.1186/1757-4749-6-14

(37) Cho, I. H.; Irudayaraj, J. In-situ Immuno-gold Nanoparticle Network ELISA Biosensors for Pathogen Detection. *Int. J. Food Microbiol.* **2013**, *164*, 70−75.

(38) Zhang, H.; Shi, Y. P.; Lan, F.; Pan, Y.; Lin, Y. K.; Lv, J. Z.; Zhu, Z. H.; Jiang, Q.; Yi, C. Detection of Single-Digit Foodborne Pathogens with the Naked Eye Using Carbon Nanotube-Based Multiple Cycle Signal Amplification. *Chem. Commun.* **2014**, *50*, 1848−1850.



DOI: 10.1021/acsami.5b11834
*ACS Appl. Mater. Interfaces* 2016, 8, 6329−6335